



**TOWARDS DEVELOPMENT APPLICATIONS BASED ON ATOMIC LAYER
DEPOSITION FOR SOLAR CELLS**

AHMED S. M. IMRAN

Department of physiology and medical Physics, College of Medicine, University of Kerbala,
56001 Karbala, Iraq

Ahmed.sadeq@uokerbala.edu.iq

Received 4th Nov. 2017; Revised 10th March 2018; Accepted 28th March 2018; Available online 1st June 2018

DOI: <https://doi.org/10.31032/IJBPAS/2018/7.6.4469>

ABSTRACT

There are a wide range of solar cell based cell advancements which go for creating power from daylight modest or potentially proficient. As the effectiveness of silicon cells is gradually yet persistently climbing, value diving, and generation soaring, there is as I would see it no place for different advances unless they can beat silicon on productivity. Business cells at more than 20 % productivity are accessible and lab cells have been accounted for at over 27 %. Contrasting this with the hypothetical most extreme productivity of a solitary intersection cell which is simply over 30 % demonstrates that we can deliver near immaculate silicon cells. Any innovation which needs to beat these needs to go for effectiveness higher than 30 %. There are not per today numerous potential contenders for this. In this paper manufacture ability in the field of light transformation and to endeavor at influencing a productive down change to film material by nuclear layer statement. Moreover, a huge piece of the work has been dedicated to promotion of science through addresses to non-logical crowds. The potential down change materials that exists in the writing normally relies upon the communication between a few distinct sorts of iotas also, frequently with the host material itself as the UV engrossing material. As ALD develops the film one sub-monolayer at once, it can give some very novel control over the nuclear dispersion all through the film. It is generally simple to switch between a few diverse cation spins freely through the statement which empowers blending of iotas that would partitioned or frame

encourages under different conditions notwithstanding the capacity to have some control of the next neighbor circulation around each sort of particle. Europium titanium oxides were picked as the model framework for this examination. This framework has the trademark glow of Eu^{3+} and solid UV ingestion of TiO_2 . Both double oxides are generally simple to blend by ALD. Thin movies of both Eu^{3+} doped anatase and shapeless $\text{Eu}_x\text{Ti}_y\text{O}_z$ was kept, while crystalline $\text{Eu}_2\text{Ti}_2\text{O}_7$ was gotten through tempering. Notwithstanding homogeneous blending, sandwich structures of isolated Eu_2O_3 and TiO_2 layers were kept. Consequently, this system gives a great chance to explore the connection between the iridescence of the material and the focus, nearby symmetry and interatomic course of action and separations. The last phase of this theory was to endeavor to make a down change material by supplanting Eu^{3+} with $\text{Yb}^{3+}/\text{Ln}^{3+}$. These lanthanide sets have been revealed in writing to part one high vitality energized state into two lower vitality energized states. In this work, vitality exchange and glow was watched, yet proficient down transformation was tragically not gotten. Be that as it may, ALD was appeared to empower some control of the course of action of the cations which could prompt down change in other material frameworks which are not effortlessly realistic by different courses.

1. INTRODUCTION

Among the substantial difficulties confronting mankind, a secure energy supply to the world's economy and society is one of the biggest. Moreover, a considerable lot of the other significant difficulties, similar to nourishment, clean drinking water and destitution is either straightforwardly or in a roundabout way identified with the vitality challenge. The IPCC's recently distributed investigate the physical science reason for environmental change appears with lucidity the effect that our general public and industry has on our atmosphere and how that thusly will have solid negative effects back on us [4]. A less

demanding to peruse synopsis of the more than 2000 page report is additionally accessible [2]. It is certain that filling our economy and society with non-renewable energy sources is exceptionally unfavorable to both on the long haul. A significant part to alleviate atmosphere changes and securing a contamination free vitality supply is an extensive scale change to sustainable energy sources [3]. From the media, it can appear as though there is a mechanical obstruction to the vast scale change to renewable like breeze and sun based and that a leap forward or something to that affect is required. Truth be told, the

advances we have accessible today are in actuality adequate, while the bottleneck is fairly the approaches and monetary motivators to actualize it [4, 6]. One noteworthy snag for renewable is that the contending petroleum products are additionally financed and diminishing these endowments is troublesome because of the substantial put interests in these enterprises [3]. Furthermore, petroleum derivative endowments are unpredictable, various and not generally effectively distinguished making it difficult to gauge it on a worldwide level [6]. It is in this way wrong to contend that renewable "depends on sponsorships", as a wide range of energy age is in truth financed somehow [8]. Specifically photovoltaic's is frequently asserted to require an achievement in either cost or effectiveness keeping in mind the end goal to be aggressive. It is contended in a current paper that this origination is both misdirecting and outdated [8]. The authors likewise contend that this misguided judgment.

To have a thought of how to enhance the productivity of sun powered cells, we first need to see how it functions and why it isn't 100 % proficient in any case. The portrayal in this section is profoundly rearranged, however ought to be sufficient for the

discourse in this theory. A significantly more exhaustive depiction of sunlight based cells can be found in the course readings by P. Würfel [15] or M. A. Green [16]. For peruses who are moderately new to the field of sun based cells and semiconductor material science, the course book by J. Nelson might be more congenial [17]. At the point when photons are caught up in a material, an electron gets eager to a higher vitality state. The point of a sun based cell is to separate this electron and change over its vitality to power. Keeping in mind the end goal to do this, two things are required by the material. To start with, the energized state (likewise called a conduction band, E_c) must be isolated (in vitality) from the beginning (additionally called a valence band, E_v) by a taboo band hole E_g . This keeps the electron from promptly unwinding back to the ground state, giving it some time to remain in the energized state. Second, the energized electron should be separate from the opening deserted in the ground state. In spite of the fact that there are more approaches to achieve this, most sunlight based solar cells this partition with a p-n intersection. At the point when an n-sort and p-type material comes in contact, a purported exhaustion district is framed at

the interface and extends a few separations into the doped areas. Inside the consumption area, there is an electric field indicating from the n-type the p-type locale. In the event that an electron gets eager to the conduction band in this area, it will be pulled towards the n-type locale by the electric field. The gap which is abandoned in the valence band will in like manner be pulled towards the p-type

district. The electron and gap are physically isolated and kept from getting back together by the electric field over the p-n intersection. Electrons gathered along these lines, or created in the n-type area, will add to an electrical current through an outer load, giving us electrical power. Figure 1 illustration showing an electron being excited from the valence band to the conduction band.

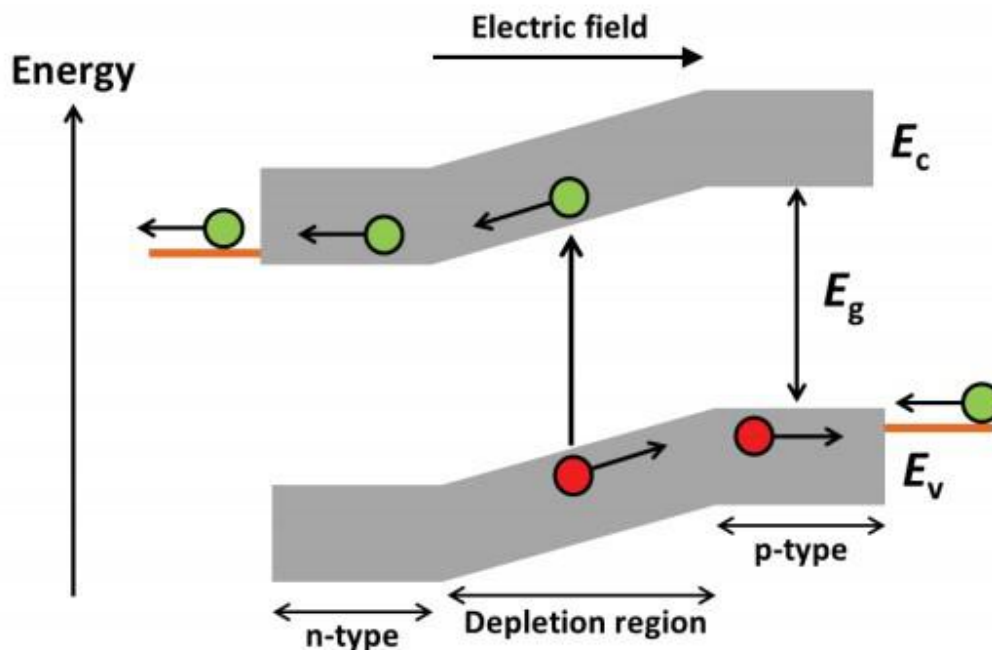


Figure 1: Illustration electron being excited from the valence band to the conduction band.

The band gap is critical with a specific end goal to give the energized electron a chance to keep up its vitality. Lamentably, it additionally puts solid constraints on which parts of the solar based range the cell can use. On the off chance that the vitality of the photon, $E\lambda$, is littler than E_g , the photon can't energize an electron starting from the earliest

stage to the energized state, and therefore won't contribute anything to the electrical current produced. Then again, if $E\lambda$ is bigger than E_g then the energized electron will rapidly unwind down to the least permitted vitality in the energized state. The surplus vitality will be discharged as phonon so the vitality is lost as warmth. This procedure is

called the realization. The daylight comprises of photons with boundlessly unique energies, as appeared in Figure 2. The band hole of silicon is 1.1 eV which compares to a photon of 1100 nm wavelength. That implies that every one of the photons with longer wavelengths can't be used to produce control, while for photons of shorter wavelength the the realization misfortune increments quickly with

diminishing wavelength. For silicon, this implies around 1/3 of the vitality of the daylight comprises of too low vitality photons to contribute and 1/3 of the vitality of the high vitality part of the range is lost as warmth, putting the hypothetically most elevated productivity at a little more than 30 %. This is additionally called the Shockley-Queisser restrain [16].

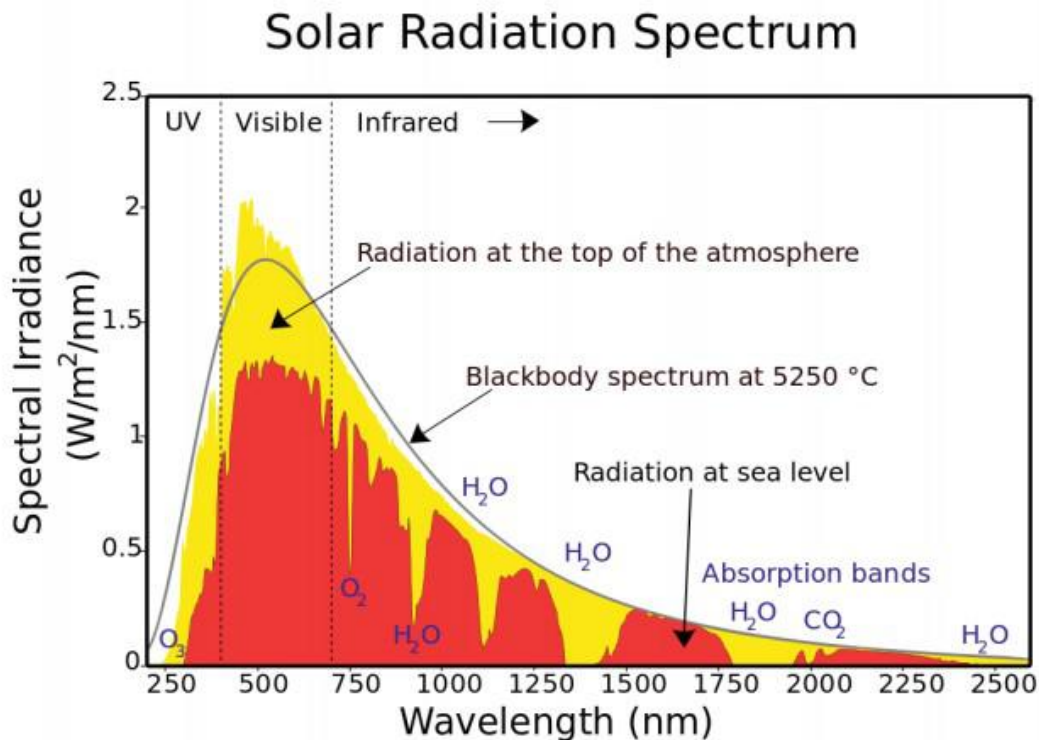


Figure 2: The solar spectrum

All in all, how well do really solar cells change over solar energy vitality into power? The National Renewable Energy Laboratory in the US have a persistently refreshed diagram * demonstrating the record efficiencies of various solar cell

advancements [20]. The lab record for non-concentrated silicon solar cells have been 25 %, set by Green et al. with a PERL cell [20]. Only as of late in April this year, Panasonic broke this record with a 25.6 % productive HIT cell [21]. Business silicon solar cells

can achieve efficiencies over 21 % [19]. As far as possible for a solitary intersection solar cell is around 30 %, this implies silicon solar cells are near great. This, alongside the way that solar cells are winding up monetarily focused an ever increasing number of spots, drives us to a couple of conclusions: 1. Silicon solar cells can be made less expensive, however not definitely more effective than they are today. 2. The two noteworthy obstructions to higher efficiencies are a) the thermalization misfortunes of the high vitality photons and b) that the sub band hole photons can't be utilized. 3. Neither of these obstructions can be conquered when consolidating a solitary intersection solar cells with the sun powered range.

2. Characterization Methods

Several characterization techniques have been used in this work. All of these techniques are however quite standard in material research and are well described in the literature. This chapter will thus only give a brief description of the different techniques and instruments used.

2.1 Spectroscopic Ellipsometry

Spectroscopic Ellipsometry is an optical reflection system which uses the distinction in reflectivity of s-and p-energized light at an interface to examine optical properties like

$n(\lambda)$ and $k(\lambda)$ and the thickness of the example. The properties of the example are found by demonstrating the estimation information. The many-sided quality of this procedure depends unequivocally on the optical multifaceted nature of the example. In this work, two ellipsometers with various range ranges was utilized and the demonstrating was finished with the Complete EASE programming, all from J. A. Woollam Co. For standard thickness estimations, an alpha-SE spectroscopic ellipsometer (390 – 900 nm) instrument was utilized. All examples are completely straightforward in this range. A Cauchy work was accordingly adequate to show the film material. To explore the UV retention properties of titania containing tests, a VASE variable point spectroscopic ellipsometer (260 – 1100 nm) instrument was utilized. To show these materials in the UV go, a Tauc-Lorentz oscillator was utilized.

2.2 Optical spectroscopy (UV-Vis-NIR)

Optical transmission estimations were led on films saved on pop lime glass in the range 180 – 3300 nm with a Shimadzu UV-3600 instrument. Three finders were utilized that cover distinctive reaches: photomultiplier tube (180 – 900 nm), InGaAs photodiode (900 – 1700 nm) and PbS photodiode (1700 – 3300 nm). All examples were exceedingly

straightforward, aside from the solid UV ingestion of the titania containing films. The feeble f-f advances were noticeable for a portion of the lanthanide oxides, while this assimilation was excessively frail, making it impossible to identify for all titania containing films.

2.3 Photoluminescence (PL)

Photoluminescence (PL) was directed on films stored on Si (100). The excitation source was a HeCd 325 nm laser while a USB4000 spectrometer from OceanOptics was utilized as a locator. The laser is spellbound as for the example surface and at an episode point of 23° while the locator was situated typical to the example surface. Tests were estimated in groups to diminish the impacts of vacillations in the laser force and so forth between the examples. At the point when another group of tests was estimated, a few examples from the past bunch were additionally estimated to have the capacity to look at tests between clumps.

2.4 X-ray diffraction (XRD)

All examples were characterized by X-beam diffraction (XRD) in θ - 2θ reflection geometry to explore the crystallinity of the stored material. A Bruker D8 Discover diffract meter with Cu $K\alpha_1$ and a Ge(111) monochromator and a LynxEye identifier was utilized for this. XRD in this geometry

can just identify gem planes parallel to the example surface. In thin film testimonies one in some cases acquires incompletely or completely situated development. Contrasted with XRD of powder tests where crystallites are haphazardly arranged, this can bring about less diffraction tops than anticipated and changes in the relative pinnacle forces. Specifically when not very many pinnacles are watched and a few stages are conceivable, deciding the crystalline phase(s) can be troublesome for thin films..

2.5 X-ray reflectivity (XRR)

The multilayer structures introduced were portrayed by X-beam reflectivity (XRR) to explore the layer structure, or deficiency in that department. A PANalytical Empyrean diffractometer with Cu radiation*, parallel shaft reflect, 0.27° parallel plate collimator and a corresponding Xe identifier was utilized for this. This system depends on the reflectivity of X-beams from materials at low occurrence points. Most materials have $n(\lambda) < 1$ in the X-beam run bringing about aggregate "inner" reflection† from the example when the occurrence point is beneath the basic edge. Hence, at edges somewhat higher than the basic point the X-beam reflectivity is at its greatest and an obstruction design is (regularly) seen between the pillars reflected from the air/test

and the example/substrate interfaces. From these examples a few example properties can be demonstrated: the thickness is identified with the wavelength of the impedance design, the harshness is identified with the hosing of the sufficiency of the obstruction design and the thickness of the film material is identified with the basic point. Every interface in multilayer structures can likewise add to the obstruction design, which is the reason XRR is very great at portraying slight multilayer structures.

2.6 X-ray fluorescence (XRF)

In X-beam fluorescence, a center electron is energized by the episode X-beam pillar. At the point when the electron unwinds down to a lower vitality orbital, X-beams are produced. These energies are particular to the orbital energies engaged with the change which are one of a kind to every component. The fluorescence range is consequently extraordinary to every component. XRF is hence a perfect non-damaging instrument to decide the basic structure of the example. Focuses down to 1 – 10 ppm can be estimated for strong examples, while for thin movies as far as possible is practically speaking more like 1 % because of the moderately little measure of test material. The X-beam fluorescence was estimated on a

Philips PW2400 instrument and dissected utilizing the UniQuant programming.

2.7 Atomic force microscopy (AFM)

Nuclear power microscopy (AFM) can be utilized to describe the surface of an example by checking the surface in a xy design with a thin needle tip and estimating the power between the tip and the surface. For indistinct materials, the helpful trademark is the surface harshness, while for crystalline examples the crystallite sizes, shapes and circulation can be pictured. In this work, a Park XE70 nuclear power magnifying instrument in tapping mode was utilized for the lanthanide oxide films while contact mode was utilized for the titanate containing films. The example region was normally a $5 \times 5 \mu\text{m}^2$ territory.

2.8 Field emission scanning electron microscopy (FESEM)

In this work, AFM has been the fundamental portrayal instrument for surface geology. One example in any case, ALD become PrOx, demonstrated hard to describe with AFM, hence field outflow checking microscopy (FESEM) was utilized for this example. FESEM is fundamentally the same as a "typical" SEM with the exemption that the cathode has been supplanted with a field outflow cathode which gives a smaller testing pillar. Practically speaking, a FESEM gives higher spatial determination than a

general SEM and have bring down necessities for the conductivity of the example as the lower electron transition in the smaller shaft causes less charging of the example surface. The FESEM portrayal on this example was improved the situation us by a designer at the FEI Corporation on NovaTM NanoSEM 650.

3. Experimental Setup

The objective of this work has been to grow thin film synthesis routes of luminescent lanthanide-based oxide materials by ALD, with the long haul point of acquiring down transformation. One of the qualities of ALD is the relative simplicity of saving multi component materials, as long as the affidavit of the double mixes is known. In this manner, this work has been a stepwise procedure. Initially, getting affidavit parameters for basic lanthanide oxides, furthermore to consolidate this with an UV retaining oxide to shape a down moving material, thirdly to examine the likelihood to make sub-nanometer layer structures, also, in conclusion to make sub-nanometer layer structures of the UV retaining oxide what's more, numerous lanthanides in the expectations of getting a down change material.

3.1 Fabrication of Deposition of lanthanide oxides

The deposition of the considerable number of lanthanides by $\text{Ln}(\text{thd})_3$ and ozone at $300\text{ }^\circ\text{C}$ have been revealed in the writing before, except for Pr and just to an exceptionally constrained degree Tb. This research work fills in the lacking information in the entire $200 - 375\text{ }^\circ\text{C}$ range and reports on the affidavit of Pr and Tb oxides. All the saved lanthanide oxides took after similar patterns, except for Pr and Tb. The patterns were: development rate expanding with temperature, indistinct at low affidavit temperatures and crystalline over a specific temperature ($250 - 300\text{ }^\circ\text{C}$ relying upon the lanthanide) and an optical retention because of f-f advances which changed as the crystallinity changed. The optical retention because of f-f advances relies upon the nearby symmetry around the lanthanide particle, what's more, in this way likewise the crystallinity or scarcity in that department. As exemplified by the Nd testimonies in Figure 18, there is a reasonable relationship between's the precious stone stage XRD reflections due to cubic Ln_2O_3 are marked with (hkl) and a reflection due to the hexagonal phase is marked "Hex.".

One intriguing outcome results here is the diverse development instruments for $\text{Pr}(\text{thd})_3$ and $\text{Tb}(\text{thd})_3$ which brought about thickness

slopes, and for $\text{Pr}(\text{thd})_3$ too an extremely organized surface originating from the higher level of crystallinity and favored introduction of these examples, Figure 4. This is likely due to these two lanthanides inclination for a blended $\text{Ln}^{3+/4+}$ state in oxide materials. The same would likely be the situation for $\text{Ce}(\text{thd})_3$ and ozone, yet past involvement with these antecedents at our gathering demonstrates that it stores as Ce^{4+} as CeO_2 which doesn't have any f electrons. In this way, this was excluded in this work. Tragically that affidavit of Pr and Tb oxides brought about blended oxidation states as $\text{Pr}^{3+}/\text{Yb}^{3+}$ and $\text{Tb}^{3+}/\text{Yb}^{3+}$ is two of the lanthanide combines most frequently demonstrating plausibility for down change in the writing. One conclusion of this work is that if unadulterated Pr^{3+} and Tb^{3+} containing materials are required, the thd and ozone process probable not appropriate.

3.2 Fabrication of Deposition of Europium Titanate

In this section, TiO_2 was picked as the UV engrossing oxide because of its affidavit by TiCl_4 and H_2O being notable in the writing. The three generally utilized lanthanides in luminescent oxides are Ce^{3+} , Eu^{3+} and Tb^{3+} . As paper I and prior encounter appeared, cerium and terbium doesn't store as unadulterated Ln^{3+} by the $\text{Ln}(\text{thd})_3/\text{ozone}$

forerunner sets, in this manner europium was picked. The movies arrangements were fluctuated by rotating between various quantities of $\text{Eu}(\text{thd})_3/\text{ozone}$ and $\text{TiCl}_4/\text{H}_2\text{O}$ cycles. The Eu – Ti oxide did to be sure luminesce, which neither TiO_2 nor Eu_2O_3 did under the same 325 nm excitation, demonstrating the vitality exchange between the TiO_2 and Eu^{3+} particles. The titanium substantial tests (< 30 % Eu_2O_3 cycles) kept as a blend of formless $\text{Eu}_x\text{Ti}_y\text{O}_z$ what's more, Eu^{3+} doped anatase, while just formless $\text{Eu}_x\text{Ti}_y\text{O}_z$ was acquired for 30 % furthermore, higher Eu_2O_3 cycles. For roughly 80 nm thick movies, the most elevated radiance was gotten for 50 % Eu_2O_3 cycles. The glow range of the undefined stage and the aggregate glow power is plotted in Figure 5. The radiance range of Eu^{3+} -doped anatase is appeared in the base range in Figure 5. The radiance range of the testimony containing in the vicinity of 10 and 20 % Eu_2O_3 cycles were superposition's of these two spectra.

I found two outcomes results acquired in this work amazing be that as it may. To begin with, the undefined stage showed significantly more grounded radiance than the crystalline $\text{Eu}_2\text{Ti}_2\text{O}_7$ stage got by tempering. The glow power of the tests diminished with expanding toughening

temperature and was for all intents and purposes zero when toughened at 700 °C. These statements demonstrated no crystalline stages by XRD, yet tests tempered at 1000 °C contained crystalline $\text{Eu}_2\text{Ti}_2\text{O}_7$ and rutile. Writing and reading material regularly give the feeling that vast single precious stones dependably give better radiance, however this is in actuality not generally obvious. Berdowski et al. discovered that crystalline $\text{Eu}_2\text{Ti}_2\text{O}_7$ demonstrate no glow at room temperature [22], while Blasse et al. discovered that glow could be seen from Eu^{3+} -doped $\text{Gd}_2\text{Ti}_2\text{O}_7$ with a similar structure. In this way, as likewise contended by these creators, it appears as though there are a solid focus extinguishing impact in this precious stone framework. Berdowski contends this is expected to the excitation exchanging between Eu^{3+} -particles until the point that it achieves an extinguishing site, as a debasement particle. Figure 6 indicates $n(\lambda)$ and $k(\lambda)$ for the toughened examples. Toughening up to and including 600 °C did not cause any change in $n(\lambda)$ and $k(\lambda)$, while higher strengthening temperatures caused an expansion in $k(\lambda)$. This backings the possibility that little crystallites, or groups, begins to shape in the indistinct material when toughening at 600 – 700 °C.

Furthermore, I expected fixation extinguishing for the europium substantial tests. This likewise did not appear to be the situation for the undefined examples, yet Or maybe the decline in glow is likely just because of the low substance of Ti^{4+} in these examples. This is in concurrence with the discoveries. The unadulterated $\text{Eu}_x\text{Ti}_y\text{O}_z$ tests additionally demonstrated an exceptionally smooth surface (RMS harshness < 0.3 nm), demonstrating that this framework has possibly great properties as an optical film material. In any case, the iridescence of these examples was extinguished by tempering, because of the arrangement of $\text{Eu}_2\text{Ti}_2\text{O}_7$. Eu^{3+} -doped nanocrystals of monoclinic $\text{La}_2\text{Ti}_2\text{O}_7$ and cubic Y-Ti-O [100] on the other hand are luminescent. Consequently, it may be conceivable to stay away from the extinguishing $\text{Eu}_2\text{Ti}_2\text{O}_7$ stage by alloying with La^{3+} or Y^{3+} which are bigger and littler in measure contrasted with Eu^{3+} .

3.3 Fabrication of Deposition of multilayer structures

In this section I have worked with layer-by-layer development of ALD would empower a controlled sub-nanometer layer structure which would later be required for the controlled blending of the Ti^{4+} and diverse Ln^{3+} particles. Keeping in mind the end goal

to examine this, the relative proportion of Eu_2O_3 and TiO_2 cycles and aggregate number of cycles was kept steady and supercycles of $N \text{ Eu}_2\text{O}_3 + N \text{ TiO}_2$ cycles were kept while fluctuating N from 1 – 50. The PL spectra shape was observed to be free of N while the aggregate PL power was relatively steady for $N = 1 - 10$ and diminished for higher N , as found in the inset in Figure 7. Indistinguishable PL spectra demonstrate that the luminescent Eu^{3+} is in a similar nearby symmetry taking all things together the examples. There were no down to earth distinction between the examples $n(\lambda)$ and $k(\lambda)$, and no precious stone stages were identified by XRD. In this manner, the real contrast between the examples ought to be

the separations and blending of the Eu^{3+} and Ti^{4+} XRR demonstrated that the $N = 10$ test did to be sure have an unmistakable layer structure. The 10 $\text{Eu}_2\text{O}_3 + 10 \text{ TiO}_2$ superlayer was observed to be 0.75 nm thick, while it was unrealistic to decide the individual Eu_2O_3 and TiO_2 layers. Be that as it may, this suggests that no less than one of the layers is under 0.4 nm thick. This is around the same as one $\text{Eu} - \text{Eu}$ separate in crystalline Eu_2O_3 . In conclusion, this implies by ALD and the $\text{Ln}(\text{thd})_3/\text{ozone} + \text{TiCl}_4/\text{H}_2\text{O}$ forerunner sets, it is conceivable to make sub-nanometer layer structures, giving a extremely one of a kind control of the spatial circulation of the distinctive cations.

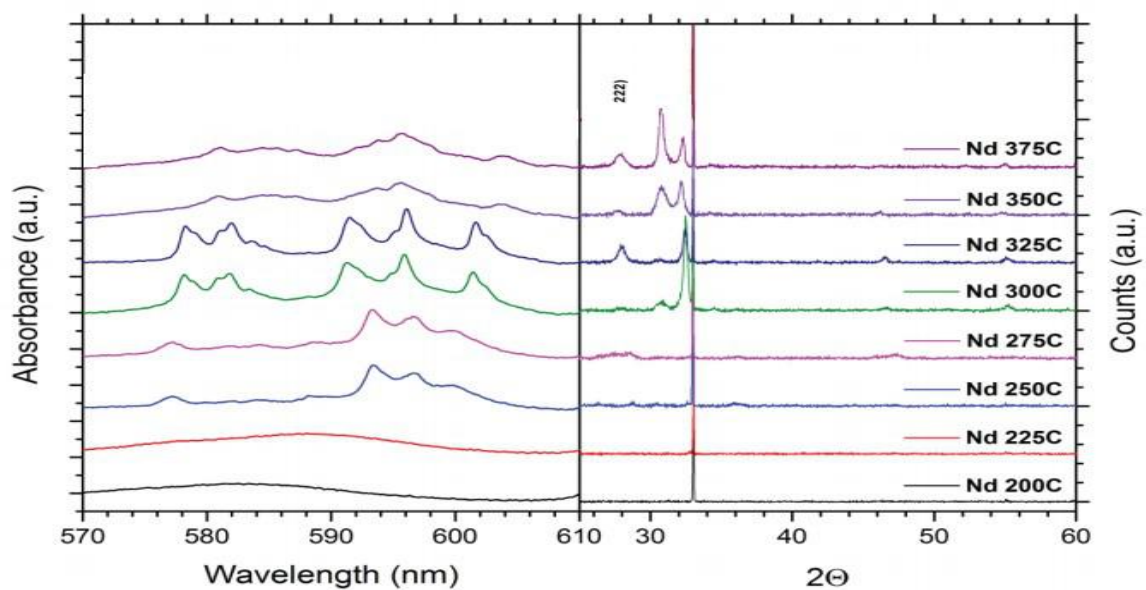


Figure 3: XRD data for the Nd_2O_3 depositions deposited at 200–375 °C (right) and optical absorbance (left) 375 °C (right).

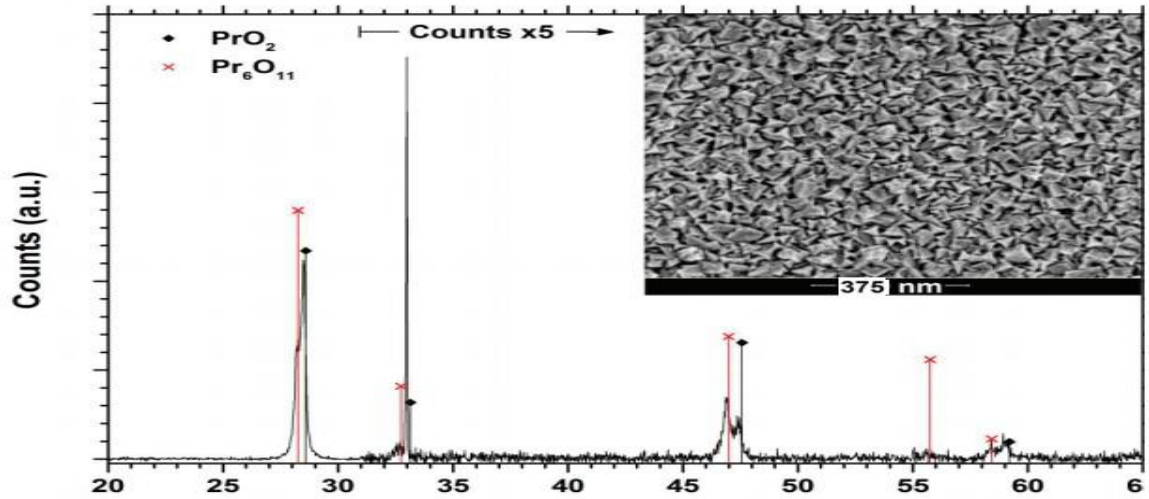


Figure 4: display the performance of XRD data and FESEM image of a Pr(thd)3 / ozone deposition at 300 °C.

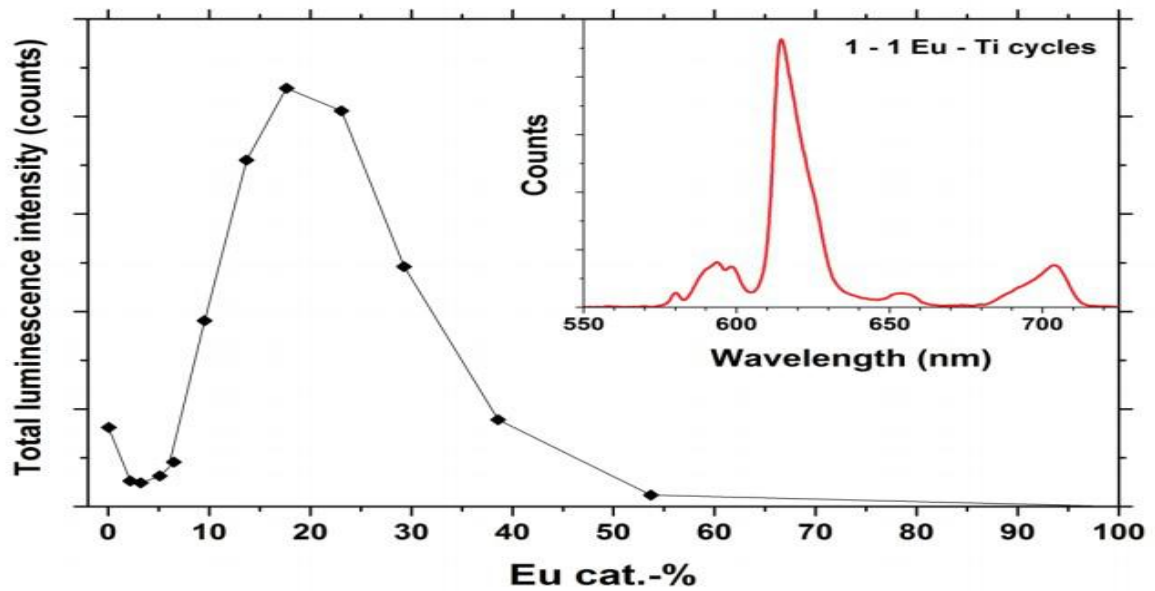


Figure 5: Depositions of 55 % cycle ratio Eu_2O_3 of Luminescence spectrum

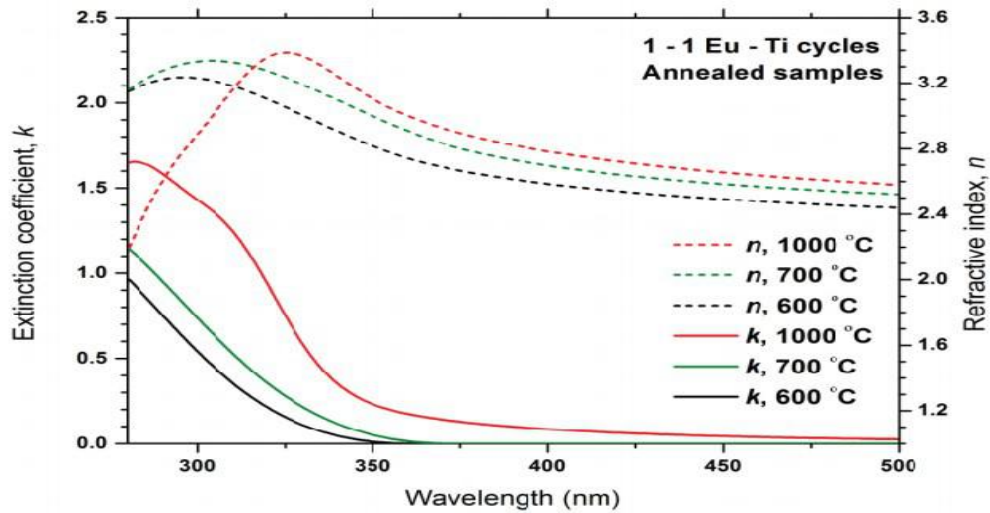


Figure 6: Depositions of alternating Eu_2O_3 and TiO_2 cycles of extinction coefficient and refractive index.

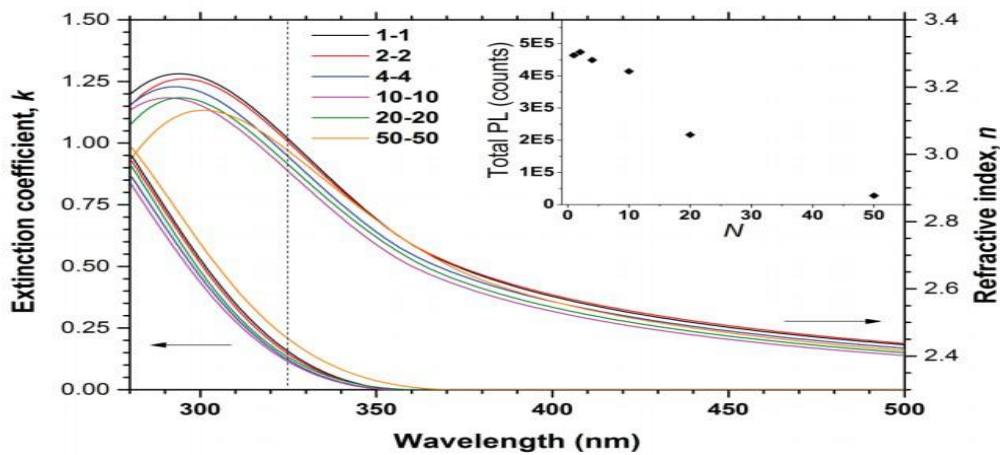


Figure 7: Display the performance of Extinction coefficient and refractive index of the layered samples

4. CONCLUSION

Down-transformation was not seen in this work. In any case, some advance has been made that demonstrate that ALD is as yet a possibly productive approach for thin film down change. The consequences of paper demonstrate that it is conceivable to control the detachment and blending of various cations down to the unit cell level. This isn't

for the most part valid for all forerunner frameworks, however having this sort of control is "essentially" an issue picking the correct antecedents. unmistakable division of the layers of under 0.4 nm is well underneath the range that the Förster vitality exchange is effective, which is when all is said in done thought to be 1 – 5 nm. In this way, controlling the nearby centralization of

various cations and which sorts of particles that are in "talking separation" to each other ought to for sure be conceivable with ALD, at any rate in the development bearing. Some control of the partition is likewise conceivable in the development plane by controlling the extent of forerunners or the number and circulation of dynamic surface locales. Maybe the biggest impediment to accomplish down transformation amid this work was the failure to deliver unadulterated Ce^{3+} , Pr^{3+} and Tb^{3+} from $Ln(thd)_3$ and ozone. These three lanthanides alongside Tm^{3+} are the most utilized accomplice to Yb^{3+} in $Ln^{3+/Yb^{3+}}$ down change sets. In this manner, as long as the procedure for acquiring down transformation is through $Ln^{3+/Yb^{3+}}$ sets, different forerunners need to be utilized. As the three tricky lanthanides effectively frames Ln^{4+} , the oxygen source must be pitifully oxidizing. Something else, and Ln^{3+} that is framed will instantly be oxidized to Ln^{4+} . This requires the lanthanide forerunner to be substantially more receptive than the $Ln(thd)_3$ mixes are. In the audit of the ALD field, no reports of unadulterated Ce^{3+} , Pr^{3+} or Tb^{3+} oxides exists starting at 2013. Another option would be the ex-situ decrease of the material. Attempts at lessening a $TbOx$ film by hydrogen at high temperatures have been made by Joachim Svendsen at our

gathering, which was unsuccessful in acquiring unadulterated Tb^{3+} . I in this manner trust that in-situ development of unadulterated Ln^{3+} is a more productive approach. A moment issue in this work is that Tm^{3+} extinguishes the Yb^{3+} discharge in the stored films. The same is likewise valid for Pr^{3+} , which no doubt contained a blend of Pr^{3+} and Pr^{4+} . In this way, maybe the $Ln_xTi_yO_z$ framework isn't appropriate for this sort of light transformation. Titanates are in certainty not extremely basic hosts for phosphor materials. Taking a gander at the phosphor writing, oxysulfide, sulfides, fluorides, vanadates and yttrium aluminum garnets are more typical materials. It may be helpful to endeavor to store these known materials to have a superior beginning stage to work with. Specifically sulfides, fluorides and different incandescent light could be useful as they are less oxidizing than oxygen so it is impossible that Ln^{4+} would exist in these hosts. While looking the writing for chips away at down transformation, a large group of distinctive materials, gem structures, smaller scale structures and particle sets is being researched all through the world. Two extra things likewise progress toward becoming obvious. One, despite the fact that there are no absence of inventiveness in the a wide range of sorts of

blend procedures detailed, they all have in like manner that the appropriation of the diverse lanthanide particles is arbitrary. The circulation of the lanthanides must be impacted by controlling the generally and relative fixations. What's more, two, no material that productively down proselytes daylight exists starting today. In this manner, I do trust that ALD can give a special field to handle the issue of creating down change materials for sun oriented cells by presenting a special control of the nuclear neighborhood. By picking better have materials more suited for luminescent materials than titanates, and picking an antecedent framework that keeps the arrangement of Ln^{4+} , ALD ought to be an appropriate blend courses for down transformation materials. Ideally, the future will tel.

REFERENCES

- [1] IPCC, Climate Change 2013: The Physical Science Basis. IPCC Fifth Assessment Report, 2013.
- [2] IPCC, Climate Change 2013: The Physical Science Basis - Summary for Policymakers. IPCC Fifth Assessment Report, 2013.
- [3] .B. Metz, O.R.D., P.R. Bosch, R. Dave, L.A. Meyer, Climate Change 2007: Mitigation of Climate Change. IPCC Fourth Assessment Report, 2007.
- [4] Jacobson, M.Z. and M.A. Delucchi, Providing all global energy with wind, water, and solar power, Part I: Technologies, energy resources, quantities and areas of infrastructure, and materials. Energy Policy, 2011. **39**(3):p.1154-1169.
- [5] Delucchi, M.A. and M.Z. Jacobson, Providing all global energy with wind, water, and solar power, Part II: Reliability, system and transmission costs, and policies. Energy Policy, 2011. **39**(3): p. 1170-1190.
- [6] Mathys, N.A., Feasibility Study for "Revealing the Scale of Subsidies to Fossil Fuels". The Global Subsidies Initiative, 2007.
- [7] Lucy Kitson, P.W., Tom Moerenhout, Subsidies and External Costs in Electric Power Generation: A comparative review of estimates. International Institute for Sustainable Development, 2011.
- [8] Bazilian, M., et al., Re-considering the economics of photovoltaic power. Renewable Energy, 2013. **53**(0): p. 329-338. REN21, Renewables 2012 Global Status Report. 2012.

- [9] Solangi, K.H., et al., A review on global solar energy policy. *Renewable and Sustainable Energy Reviews*, 2011. **15**(4): p. 2149-2163.
- [10] Moosavian, S.M., et al., Energy policy to promote photovoltaic generation. *Renewable and Sustainable Energy Reviews*, 2013. **25**(0): p.44-58. IPCC, *Renewable Energy Sources and Climate Change Mitigation. Special Report of the Intergovernmental Panel on Climate Change*, 2012.
- [11] Tsoutsos, T., N. Frantzeskaki, and V. Gekas, Environmental impacts from the solar energy technologies. *Energy Policy*, 2005. **33**(3): p. 289-296.
- [12] Jäger-Waldau, A., *Research, Solar Cell Production and Market Implementation of Photovoltaics. PV Status Report 2012*, 2012.
- [13] Würfel, P., *Physics of Solar Cells: From Principles to New Concepts*. 2005: WILEY-VCH Verlag GmbH & Co.
- [14] Green, M.A., *Solar Cells: Operating Principles, Technology, and System Applications*. 1992: University of New South Wales.
- [15] Nelson, J., *The Physics of Solar Cells*. 2003: Imperial College Press.
18. Shockley, W. and H.J. Queisser, Detailed Balance Limit of Efficiency of p-n Junction Solar Cells. *Journal of Applied Physics*, 1961. **32**(3): p. 510-519.
- [16] Nick84. http://commons.wikimedia.org/wiki/File:Solar_spectrum_en.svg. Wikimedia Commons 2013, Accessed 25/10/2013.
- [17] NREL. http://www.nrel.gov/ncpv/images/efficiency_chart.jpg. Accessed 26/03/2014.
- [18] Panasonic. Panasonic HIT® Solar Cell Achieves World's Highest Energy Conversion Efficiency of 25.6% at Research Level. Accessed 25/10/2013.
- [19] Sun Power. Accessed 25/10/2013. <http://us.sunpowercorp.com/homes/products-services/solarpanels/x-series/>.
- [20] Klampaftis, E., et al., Enhancing the performance of solar cells via luminescent down-shifting of the incident spectrum: A review. *Solar Energy Materials and Solar Cells*, 2009. **93**(8): p. 1182-1194.

[21] Chen, J.Y., et al., Efficiency improvement of Si solar cells using metalenhanced nanophosphor fluorescence. *Solar Energy Materials and Solar Cells*, 2014. **120, Part A(0)**: p. 168-174.

[22] Trupke, T., M.A. Green, and P. Würfel, Improving solar cell efficiencies by down-conversion of high-energy photons. *Journal of Applied Physics*, 2002. **92(3)**: p. 1668-1674.